Silver(I)−Polynitrile Network Solids for Anion Exchange: Anion-Induced Transformation of Supramolecular Structure in the Crystalline State

Kil Sik Min and Myunghyun Paik Suh*

Contribution from the School of Chemistry & Molecular Engineering and Center for Molecular Catalysis, Seoul National University, Seoul 151-742, Republic of Korea

Received February 22, 2000

Abstract: Novel supramolecular solids whose topologies depend on the counteranion, $[Ag(C_{14}H_{20}N_6)(NO_3)]$ (**1**), $[Ag(C_{14}H_{20}N_6)]CF_3SO_3$ (**2**), and $[Ag(C_{14}H_{20}N_6)]ClO_4$ (**3**), have been prepared by the self-assembly of AgX (X = NO_3^-, $CF_3SO_3^-$, and ClO_4^-) with ethylenediaminetetrapropionitrile (EDTPN, $C_{14}H_{20}N_6$). X-ray crystal structures indicate that compounds **1**−**3** are a 1-D coordination polymer, a 2-D layer, and a boxlike 2-D network, respectively. In **1**, **2**, and **3**, the EDTPN ligand undergoes anion-dependent ligation to bind two, three, and five Ag(I) ions per EDTPN, respectively, by using the cyano groups in addition to two tertiary nitrogen atoms. The coordination numbers of Ag(I) ion in **1**, **2**, and **3**, are five, four, and six, respectively. Interestingly, the $CF_3SO_3^-$ anion of **2** is exchanged with NO_3^- and ClO_4^- quantitatively in the crystalline state when the crystal of **2** is immersed in the aqueous solutions of $NaNO_3$ and $NaClO_4$, respectively. The anion-exchange process is reversible between **1** and **2** but irreversible from **1** or **2** into **3**. The supramolecular structural transformations among **1**−**3** are observed in the crystalline state, concomitant with the anion-exchange.

Introduction

Self-assembly of metal-based supramolecules has attracted considerable interest because of the potential ability for selective inclusion and transportation of ions and molecules and the catalysis for specific chemical reactions.[1−8] An exciting, yet little explored area of supramolecular chemistry is the interconversion between different structures by the input of external information such as protons, electrons, and anions. Such supramolecules may have functional use due to their switching ability and the possibility to sequester and release guest molecules. In addition, the control of the dimensionality is also a challenge in the metal coordination polymer field since the ancillary ligation by solvent or anion may result in low dimensionality even with the polyfunctional ligands. The assembly of supramolecular solids that can sequester nitrate anion is important since a great amount of nitrate has been found in radioactive tank wastes from certain nuclear power plants,[9] and it is also involved in groundwater contamination to cause high incidences of methemoglobinemia[10] and non-Hodgkin's lymphomas.[11,12]

Here, we present novel supramolecular solids $[Ag(C_{14}H_{20}N_6)(NO_3)]$ (**1**), $[Ag(C_{14}H_{20}N_6)]CF_3SO_3$ (**2**), and $[Ag(C_{14}H_{20}N_6)]ClO_4$ (**3**), whose topologies and dimensionality depend on the counteranion. They were obtained by the self-assembly (Scheme 1) of AgX (X = NO_3^-, $CF_3SO_3^-$, and ClO_4^-) and ethylenediaminetetrapropionitrile (EDTPN, $C_{14}H_{20}N_6$). The solid **2** can be used as the nitrate-sequestering agent since quantitative and reversible anion-exchange with nitrate is possible. Moreover, the structural transformations in the crystalline state among **1**−**3** were observed concomitant with the ion-exchange.

Experimental Section

General Methods. All chemicals and solvents used in the synthesis were of reagent grade and used without further purification. Ethylenediaminetetrapropionitrile (EDTPN) was prepared according to the literature method previously reported.[13] Infrared spectra were recorded with a Perkin-Elmer 2000 FT-IR spectrophotometer. Elemental analyses (EA) were performed by the analytical laboratory of Seoul National University. X-ray powder diffraction (XRPD) data were recorded on a Mac Science M18XHF-22 diffractometer at 50 kV and 100 mA for

(1) (a) Lehn, J.-M. *Supramolecular Chemistry*: *Concepts and Perspectives*; VCH Publishers: Weinheim, Germany, 1995. (b) Amabilino, D. B.; Stoddart, J. F. *Chem. Rev.* **1995**, *95*, 2725. (c) Lawrence, D. S.; Jiang, T.; Levett, M. *Chem. Rev.* **1995**, *95*, 2229. (d) Iwamoto, T. *Inclusion Compounds*; Atwood, J. L., Davies, J. E. D., MacNicol, D. D., Eds.; Academic Press: London, 1991; Vol. 5, Chapter 6, pp 177−212.

(2) Gudbjartson, H.; Biradha, K.; Poirier, K. M.; Zaworotko, M. J. *J. Am. Chem. Soc*. **1999**, *121*, 2599.

(3) (a) Dewa, T.; Endo, K.; Aoyama, Y. *J. Am. Chem. Soc*. **1998**, *120*, 8933. (b) Sawaki, T.; Dewa, T.; Aoyama, Y. *J. Am. Chem. Soc*. **1998**, *120*, 8539.

(4) Fujita, M.; Aoyagi, M.; Ibukuro, F.; Ogura, K.; Yamaguchi, K. *J. Am. Chem. Soc*. **1998**, *120*, 611.

(5) Olenyuk, B.; Whiteford, J. A.; Fechtenkötter, A.; Stang, P. J. *Nature* **1999**, *398*, 796.

(6) (a) Munakata, M.; Wu, L. P.; Yamamoto, M.; Kuroda-Sowa, T.; Maekawa, M. *J. Am. Chem. Soc*. **1996**, *118*, 3117. (b) Munakata, M.; Wu, L. P.; Ning, G. L.; Kuroda-Sowa, T.; Maekawa, M.; Suenaga, Y.; Maeno, N. *J. Am. Chem. Soc*. **1999**, *121*, 4968.

(7) Kondo, M.; Yoshitomi, T.; Seki, K.; Matsuzaka, H.; Kitagawa, S. *Angew. Chem., Int. Ed. Engl.* **1997**, *36*, 1725.

(8) (a) Li, H.; Davis, C. E.; Groy, T. L.; Kelley, D. G.; Yaghi, O. M. *J. Am. Chem. Soc*. **1998**, *120*, 2186. (b) Li, H.; Eddaoudi, M.; Richardson, D. A.; Yaghi, O. M. *J. Am. Chem. Soc*. **1998**, *120*, 8567. (c) Li, H.; Eddaoudi, M.; Groy, T. L.; Yaghi, O. M. *J. Am. Chem. Soc*. **1998**, *120*, 8571.

(9) "Facts About Hanford", First Hanford Separation Science Workshop, July 23−25, 1991.

(10) Canter, L. W. *Nitrates in Groundwater*; CRC Press: Boca Raton, FL, 1997.

(11) Weisenburger, D. D. *Nitrate Contamination*: *Exposure*, *Consequence*, *Control*; Bogárdi, I., Kuzelka, R. D., Eds.; Springer-Verlag: New York, 1991; p 309.

(12) Mason, S.; Clifford, T.; Seib, L.; Kuczera, K.; Bowman-James, K. *J. Am. Chem. Soc*. **1998**, *120*, 8899.

(13) Buhleier, E.; Wehner, W.; Vögtle, F. *Synthesis* **1978**, 155.

10.1021/ja000642m CCC: $19.00
Published on Web 07/08/2000

Scheme 1

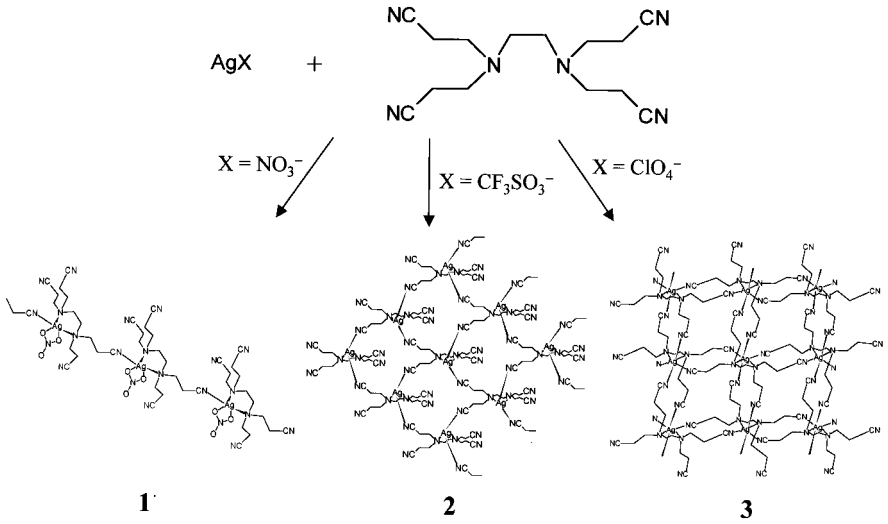

Cu Kα (λ = 1.54050 Å) with a scan speed of 5°/min and a step size of 0.02° in 2θ. Thermogravimetric analysis (TGA) and differential scanning calorimetry (DSC) were performed at a scan rate of 5 °C/min using a DuPont TGA 2050 TA instrument and a DuPont DSC 2100 TA instrument, respectively.

[Ag($C_{14}H_{20}N_6$)(NO_3)] (1). A MeOH (5 mL) solution of $AgNO_3$ (0.16 g, 0.92 mmol) was added dropwise to the MeOH solution (30 mL) of ethylenediaminetetrapropionitrile (0.25 g, 0.92 mmol) at room temperature. The solution was allowed to stand in a refrigerator until colorless crystals formed, which were filtered off, washed with MeOH, and dried in air. Yield: 90%. Anal. Calcd for $AgC_{14}H_{20}N_7O_3$: C, 38.02; H, 4.56; N, 22.17. Found: C, 37.84; H, 3.99; N, 21.99. FT-IR (Nujol mull, cm^{-1}): 2259 (s), 2250 (s), 1421 (s), 1303 (s), 1168 (m), 1121 (s), 1100 (s), 1035 (s), 997 (m), 984 (s), 952 (s), 816 (s), 771 (s), 756 (s), 723 (s), 621 (s).

[Ag($C_{14}H_{20}N_6$)]X (X = $CF_3SO_3^-$ for 2, X = ClO_4^- for 3). A MeOH (5 mL) solution of AgX (0.92 mmol) was added dropwise to the MeOH solution (30 mL) of ethylenediaminetetrapropionitrile (0.25 g, 0.92 mmol) at room temperature. The solution was allowed to stand in a refrigerator until colorless crystals formed, which were filtered off, washed with MeOH, and dried in air. Yield: 90%. Anal. Calcd for $AgC_{15}H_{20}N_6O_3F_3S$ (**2**): C, 34.04; H, 3.81; N, 15.88; S, 6.06. Found: C, 34.01; H, 3.57; N, 15.96; S, 6.22. FT-IR (Nujol mull, cm^{-1}): 2284 (s), 2252 (s), 1421 (s), 1263 (s), 1223 (s), 1148 (s), 1099 (s), 1030 (s), 984 (s), 965 (m), 941 (s), 810 (m), 753 (s), 722 (m), 636 (s), 571 (s). Anal. Calcd for $AgC_{14}H_{20}N_6ClO_4$ (**3**): C, 35.06; H, 4.20; N, 17.52. Found: C, 34.94; H, 4.38; N, 17.89. FT-IR (Nujol mull, cm^{-1}): 2264 (s), 2248 (sh), 1455 (s), 1419 (s), 1367 (s), 1298 (m), 1281 (m), 1127 (s), 1086 (s), 977 (s), 814 (s), 623 (s).

Ion Exchange in the Solid State. A freshly prepared rodlike crystal of **2** (0.25 g) was immersed in the aqueous solution of $NaNO_3$ (3 or 0.1 M, 5 mL) for 10 min to 24 h. The transparency of the crystal was lost during the immersion. The resulting anion-exchanged solid was filtered off, washed several times with water, and then dried in air. The product was characterized by EA, FT-IR spectra, and XRPD pattern. To verify the reversible anion-exchange, the anion-exchanged solid was immersed in 3 M $LiCF_3SO_3$, filtered off, washed several times with water, dried, and then identified by EA, FT-IR spectra, and XRPD. Similar experiments were performed with the crystal of **2** by immersing it in 3 M aqueous solutions of $NaNO_3$, $LiCF_3SO_3$, $NaClO_4$, NaCl, and in the solution of 2 M $NiSO_4$. The same experiments were also performed with the crystals of **1** and **3** (0.20 g). The ion-exchange experiments were also carried out in 0.1−0.01 M $NaNO_3$, 0.1−0.01 M $LiCF_3SO_3$, and 0.1−0.001 M $NaClO_4$, where the solids were immersed for a few days, and the products were filtered off, washed several times with water, dried, and then identified by FT-IR spectra.

X-ray Diffraction Measurements. Single crystals of **1**−**3** were mounted on an Enraf-Nonius CAD4 diffractometer. The unit cell parameters were determined from 25 machine-centered reflections with $22 \le 2\theta \le 28°$ for **1**, $22 \le 2\theta \le 26°$ for **2**, and $22 \le 2\theta \le 29°$ for **3**. Intensities were collected with graphite-monochromated Mo Kα radiation, using the $\omega-2\theta$ scan. Three standard reflections were measured every 2 h as orientation and intensity control and no significant intensity decay was observed. Lorentz and polarization corrections were made. No absorption correction was made. The crystal structures were solved by the direct methods[14] and refined by full-matrix least-squares refinement using the SHELXL97 computer program.[15] The positions of all non-hydrogen atoms were refined with anisotropic displacement factors. In **2** and **3**, the counteranions $CF_3SO_3^-$ and ClO_4^-, respectively, were found more or less disordered. The hydrogen atoms were allowed to ride on their bonded atoms with the isotropic displacement factors fixed with values of 1.2 times those of the bonded atoms. The crystallographic data of **1**−**3** are summarized in Table 1.

Results and Discussion

Self-Assembly. Colorless crystals of **1**, **2**, and **3** were prepared from AgX (X = NO_3^-, $CF_3SO_3^-$, and ClO_4^-, respectively) and ethylenediaminetetrapropionitrile (EDTPN) in MeOH. Although the stoichiometry (1:1) of Ag(I)/EDTPN in **1**−**3** is same, their topologies are different. As shown in Scheme 1, the coordination number of Ag(I) ion as well as the network structures in **1**−**3** depend on the anion. The coordination numbers of Ag(I) ion in **1**−**3** are five, four, and six, respectively. The topologies of **1**−**3** are a 1-D chain, a 2-D layer, and a boxlike 2-D network, respectively. Compounds **1**−**3** are insoluble in water, acetone, and MeOH, but soluble in Me_2SO. The ν(CN) values of EDTPN for **1**−**3** are summarized in Table 2. In general, coordinated nitrile shows higher CN stretching frequency than the uncoordinated.[16] TGA and DSC traces of **1**−**3** (Figures S1−S3) indicate that the compounds are thermally stable up to 140 °C.

X-ray Crystal Structure of 1. An ORTEP view of [Ag($C_{14}H_{20}N_6$)(NO_3)] (**1**) is shown in Figure 1a. Table 3 shows the selected bond distances and angles. In the structure, silver(I) ion is coordinated with two tertiary nitrogens of an EDTPN and two oxygen atoms of nitrate anion as well as one cyano group of EDTPN whose two tertiary nitrogens coordinate

(14) Sheldrick, G. M. *Acta Crystallogr*. **1990**, *A46*, 467.
(15) Sheldrick, G. M. SHELXL97. Program for the crystal structure refinement; University of Göettingen, Göettingen, Germany, 1997.
(16) (a) Nakamoto, K. *Infrared and Raman Spectra of Inorganic and Coordination compounds*, 5th ed.; John Wiley & Sons: New York, 1997; Part B, p 105. (b) Suh, M. P.; Shim, B. Y.; Yoon, T.-S. *Inorg. Chem*. **1994**, *33*, 5509.

Table 1. Crystallographic Data for $[Ag(C_{14}H_{20}N_6)(NO_3)]$ (**1**), $[Ag(C_{14}H_{20}N_6)]CF_3SO_3$ (**2**), and $[Ag(C_{14}H_{20}N_6)]ClO_4$ (**3**)

	1	**2**	**3**
formula	$AgC_{14}H_{20}N_7O_3$	$AgC_{15}H_{20}N_6O_3F_3S$	$AgC_{14}H_{20}N_6ClO_4$
fw	442.24	529.30	479.68
crystal system	monoclinic	monoclinic	orthorhombic
space group	$P2_1/c$	$P2_1/n$	$Pccn$
a, Å	7.785(1)	10.563(1)	11.050(3)
b, Å	17.781(3)	17.186(2)	11.414(3)
c, Å	13.173(3)	11.470(1)	14.790(4)
β, deg	91.53(1)	90.14(1)	
V, Å^3	1822.7(5)	2082.2(3)	1865.4(8)
Z	4	4	4
ρ_{calc}, g/cm^3	1.612	1.688	1.708
temperature	room temp	room temp	room temp
λ, Å	0.71069	0.71069	0.71069
μ, mm^{-1}	1.134	1.123	1.256
GOF	0.977	0.969	1.007
$F(000)$	896	1064	968
no. of data collcd	3431	3352	1606
no. of unique data	3142	3106	1567
no. of obsd data $[F > 4\sigma(F)]$	2378	2396	1314
no. of variables	226	262	125
R_1[a]	0.0387 (4σ data)	0.0471 (4σ data)	0.0545 (4σ data)
R_2[b]	0.0925 (4σ data)	0.1170 (4σ data)	0.1455 (4σ data)

[a] $R_1 = \sum||F_o| - |F_c||/\sum|F_o|$. [b] $R_2 = [\sum[w(|F_o|^2 - |F_c|^2)^2]/\sum[w(|F_o|)^4]^{1/2}$. $w = 1/[\sigma^2(F_o^2) + (0.0645P)^2]$, where $P = (F_o^2 + 2F_c^2)/3$ for **1**. $w = 1/[\sigma^2(F_o^2) + (0.0986P)^2]$, where $P = (F_o^2 + 2F_c^2)/3$ for **2**. $w = 1/[\sigma^2(F_o^2) + (0.1075P)^2 + 2.3722P]$, where $P = (F_o^2 + 2F_c^2)/3$ for **3**.

Table 2. IR Spectral Data for **1**, **2**, and **3**

compound	$\nu_{\text{coordinated CN}}$,[a] cm^{-1}	$\nu_{\text{free CN}}$,[a] cm^{-1}	ν_{anion},[a] cm^{-1}
1	2259	2250	1303
2	2284	2252	1263
3	2264		1086

[a] Measured with Nujol mulls.

neighboring Ag(I) ion. The Ag−$N_{tertiary}$ and Ag−N_{cyano} bond distances are 2.433(2) and 2.346(4) Å, respectively. For the coordinated nitrate anion, two Ag−O bond distances are 2.344(4) and 2.634(4) Å, respectively, and the bond angle of O1−N7−O2 is 115.6(4)°, which is smaller than the angles involving the free oxygen atom of nitrate (∠O1−N7−O3 = 122.4(4)°, ∠O2−N7−O3 = 122.1(4)°). The coordination geometry around Ag(I) is best described as a distorted trigonal bipyramid. Each EDTPN links two Ag(I) ions since three of four cyano groups of the ligand remain free and only one cyano group coordinates a neighboring silver(I) ion. Therefore, the structure of **1** becomes a linear coordination polymer, which extends parallel to the *a* axis. The separation of Ag···Ag within a chain is 7.785 Å (Figure 1b). The shortest interchain Ag···Ag distance is 5.625 Å.

X-ray Crystal Structure of 2. An ORTEP drawing of the cation in **2** is represented in Figure 2a. Table 4 shows the selected bond distances and angles. The silver ion displays tetrahedral coordination geometry, coordinated with two tertiary amines of EDTPN with an average Ag−N distance of 2.424(2) Å and two cyano groups from two different EDTPN belonging to the neighboring silver(I) ions with an average Ag−N distance of 2.248(3) Å. As each EDTPN ligand binds three different Ag(I) ions and each Ag(I) is linked with three EDTPN (Figure 2b), whole structure becomes a 2-D layer. The basic motif of a 2-D cationic layer is the rhombic ring which is composed of 22 atoms including three Ag(I) ions. The layer is markedly ruffled and propagates along the *ac* plane. The shortest Ag···Ag distance within a layer is 7.946 Å. The layers are stacked in a staggered manner and repeated with the ··ABABAB·· sequence. The two layers including Ag(I) ions are separated by 8.593 Å. The shortest interatomic distance between two layers is 3.397 Å. The triflate ions do not coordinate Ag(I) ions and locate

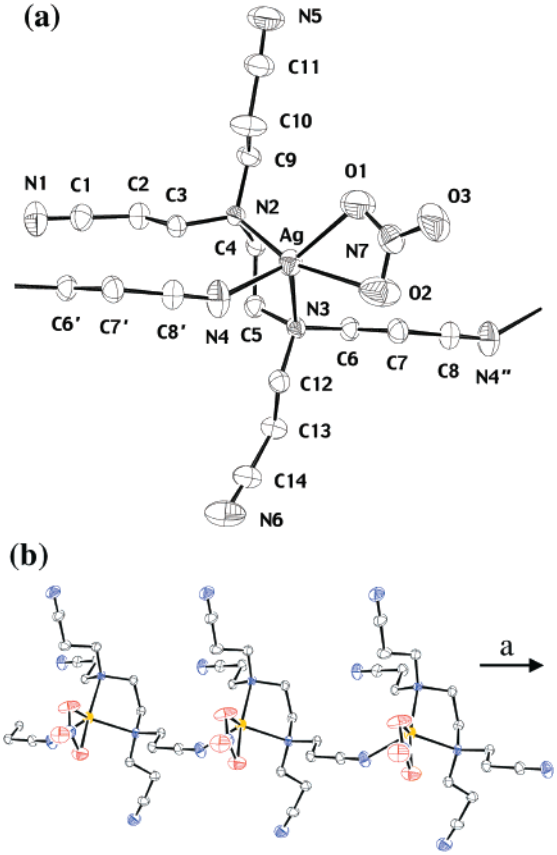

Figure 1. (a) ORTEP drawing of $[Ag(C_{14}H_{20}N_6)(NO_3)]$ (**1**) showing the local coordination of Ag(I) and the atomic numbering scheme. The atoms are represented by 40% probable thermal ellipsoid. (b) Extended 1-D structure of **1** (yellow, silver ion; blue, nitrogen; black, carbon; red, oxygen).

between the layers (Figure 2c). They show F···H−C hydrogen-bonding interactions:[17] F1···C4(x, y, z − 1), 3.384 Å; F1···H4A(x, y, z − 1), 2.582 Å; ∠F3···H4A−C4, 140.1°; F3···C13(x,

(17) Thalladi, V. R.; Weiss, H.-C.; Blaser, D.; Boese, R.; Nangia, A.; Desiraju, G. R. *J. Am. Chem. Soc.* **1998**, *120*, 8702.

Table 3. Selected Bond Distances (Å) and Angles (deg) for $[Ag(C_{14}H_{30}N_6)(NO_3)]$ (**1**)[a]

Ag−O1	2.344(4)	N6−C14	1.128(6)
Ag−O2	2.634(4)	C1−C2	1.444(6)
Ag−N2	2.436(3)	C2−C3	1.543(5)
Ag−N3	2.429(3)	C4−C5	1.519(5)
Ag−N4	2.346(4)	C6−C7	1.515(5)
N1−C1	1.139(6)	C7−C8	1.453(6)
N2−C3	1.463(5)	C9−C10	1.514(6)
N2−C4	1.492(5)	C10−C11	1.457(6)
N2−C9	1.477(5)	C12−C13	1.542(5)
N3−C5	1.481(5)	C13−C14	1.461(7)
N3−C6	1.464(5)	N7−O1	1.228(5)
N3−C12	1.466(5)	N7−O2	1.227(5)
N4−C8′	1.137(5)	N7−O3	1.220(5)
N5−C11	1.126(6)		
O1−Ag−N2	116.16(12)	N2−Ag−N3	78.42(10)
O1−Ag−N3	135.17(15)	N2−Ag−N4	102.69(12)
O1−Ag−N4	110.16(17)	N3−Ag−N4	106.76(13)
O1−Ag−O2	48.89(12)	C3−N2−Ag	107.8(2)
O2−Ag−N2	161.08(12)	C3−N2−C4	112.4(3)
O2−Ag−N3	104.38(12)	C3−N2−C9	113.3(3)
O2−Ag−N4	94.47(14)	C4−N2−Ag	101.0(2)
C4−N2−C9	109.0(3)	N3−C6−C7	112.0(3)
C9−N2−Ag	112.7(2)	C6−C7−C8	111.2(3)
C6−N3−C12	113.1(3)	N4−C8′−C7′	178.6(5)
C6−N3−C5	110.1(3)	N2−C9−C10	110.9(3)
C12−N3−C5	111.4(3)	C9−C10−C11	111.7(4)
C6−N3−Ag	114.3(2)	N5−C11−C10	178.1(6)
C12−N3−Ag	103.6(2)	N3−C12−C13	115.8(3)
C5−N3−Ag	103.7(2)	C14−C13−C12	109.9(4)
C8′−N4−Ag	151.1(4)	N6−C14−C13	175.9(5)
N1−C1−C2	178.8(5)	O1−N7−O2	115.6(4)
C1−C2−C3	111.2(3)	O1−N7−O3	122.4(4)
N2−C3−C2	115.7(3)	O2−N7−O3	122.1(4)
N2−C4−C5	112.9(3)	N7−O1−Ag	105.1(3)
N3−C5−C4	112.1(3)		

[a] Symmetry transformations used to generate equivalent atoms: prime, $x - 1, y, z$.

$y, z - 1$), 3.452 Å; F13···H13B($x, y, z - 1$), 2.656 Å; ∠F3···H13A−C13, 139.5°.

X-ray Crystal Structure of 3. An ORTEP view of the cation in **3** is shown in Figure 3a. Table 5 shows the selected bond distances and angles. The silver(I) ion displays octahedral coordination geometry, coordinated with two tertiary nitrogens of an EDTPN and four cyano groups of EDTPN belonging to four different neighboring Ag(I) ions. Each Ag(I) ion is coordinated with five EDTPN ligands, and each EDTPN links five Ag(I) ions, which gives rise to a boxlike 2-D network as shown in Figure 3b. The $Ag-N_{tertiary}$, $Ag-N_{cyano}$(equatorial), and $Ag-N_{cyano}$(axial) bond distances are 2.526(3), 2.369(4), and 2.762(6) Å, respectively. The 2-D layers propagate along the *ab* plane. The layers are separated by the distance of 0.5*c* of cell parameter and stacked in the staggered manner with the ··ABABAB·· sequence. The shortest intrasheet and intersheet Ag···Ag distances are 7.982 and 7.395 Å, respectively. The perchlorate ions are not coordinated to the Ag(I) ions and occupy the space between the layers (Figure 3c). They show C−H···O hydrogen-bonding interactions:[17] O3···C5, 3.439 Å; O3···H5B, 2.558 Å; ∠O3···H5B−C5, 151.0°.

Anion Exchange of Supramolecular Solids and Structural Transformation in the Crystalline State. When the insoluble crystal of **2** was immersed in an aqueous solution of 3 M $NaNO_3$ for 1 h or 0.1 M $NaNO_3$ for 10 h, the $CF_3SO_3^-$ anion of the crystal was quantitatively exchanged with NO_3^-. During the ion-exchange, the crystal maintained the crystalline state although its transparency was lost. The product was identified by EA[18] and the FT-IR spectrum as well as the XRPD pattern.

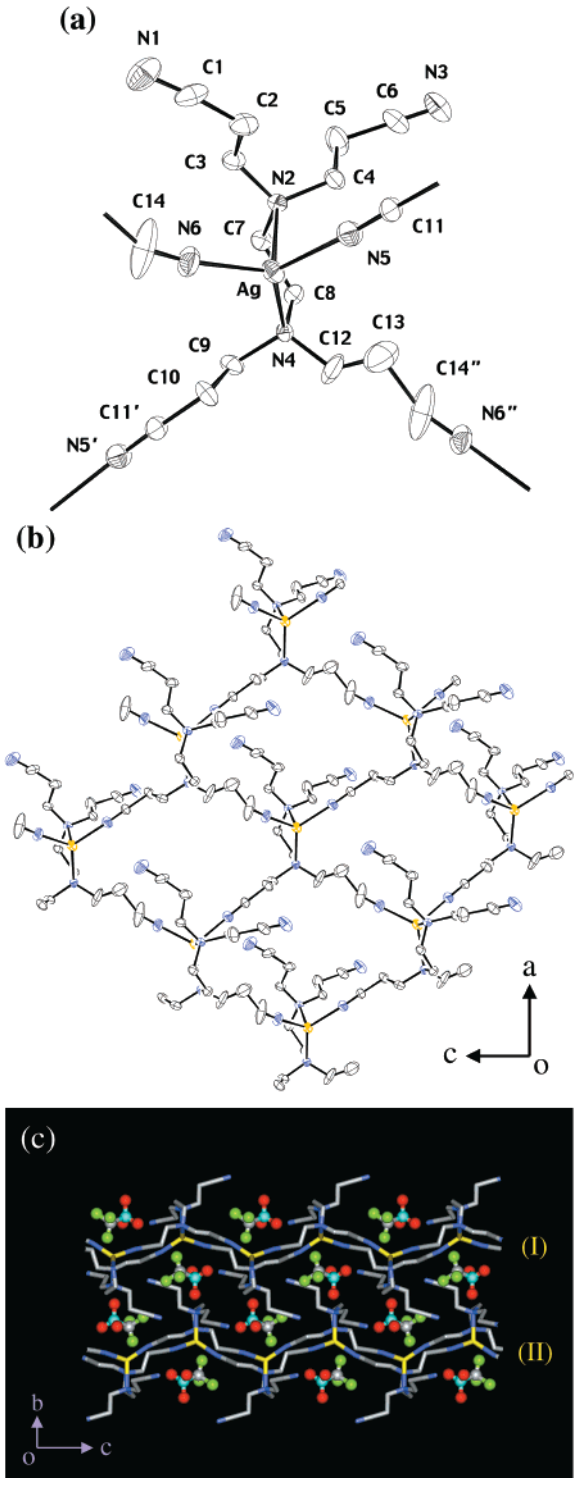

Figure 2. (a) ORTEP drawing of cation of **2** showing the local coordination of Ag(I) and the atomic numbering scheme. The atoms are represented by 25% probable thermal ellipsoid. (b) Extended 2-D structure of **2** (yellow, silver ion; blue, nitrogen; black, carbon). (c) Side view of the packed structure of **2**, showing the position of $CF_3SO_3^-$ ions (yellow, silver ion; blue, nitrogen; gray, carbon; red, oxygen; sky blue, sulfur; green, fluorine). The two different series of 2-D layers are indicated as **I** and **II**.

The XRPD of the ion-exchanged product was fully coincident with that of **1** as prepared from $AgNO_3$ and EDTPN (Figure 4), indicating that the structure of **2** was converted to that of **1** by the anion-exchange of $CF_3SO_3^-$ for NO_3^-. However, the

(18) Anal. Calcd for $AgC_{14}H_{20}N_7O_3$: C, 38.02; H, 4.56; N, 22.17. Found: C, 37.72; H, 3.80; N, 22.06. $\nu(NO_3^-)$: 1306 cm^{-1}.

Table 4. Selected Bond Distances (Å) and Angles (deg) for $[Ag(C_{14}H_{30}N_6)]CF_3SO_3$ (**2**)[a]

Ag−N2	2.458(3)	C2−C3	1.531(6)
Ag−N4	2.364(4)	C4−C5	1.526(7)
Ag−N5	2.243(4)	C5−C6	1.516(8)
Ag−N6	2.252(4)	C7−C8	1.521(6)
N1−C1	1.188(9)	C9−C10	1.532(7)
N2−C3	1.454(6)	C10−C11′	1.451(6)
N2−C4	1.475(5)	C12−C13	1.213(14)
N2−C7	1.481(5)	C13−C14″	1.619(14)
N3−C6	1.092(7)	S1−O1	1.348(8)
N4−C12	1.436(7)	S1−O3	1.360(6)
N4−C8	1.477(6)	S1−O2	1.364(8)
N4−C9	1.493(5)	S1−C15	1.716(13)
N5−C11	1.136(6)	C15−F1	1.244(10)
N6−C14	1.109(8)	C15−F2	1.277(12)
C1−C2	1.404(9)	C15−F3	1.522(19)
N2−Ag−N4	78.66(12)	N5−Ag−N6	105.54(19)
N2−Ag−N5	98.01(15)	C3−N2−C4	113.9(3)
N2−Ag−N6	113.33(16)	C3−N2−C7	111.7(3)
N4−Ag−N5	124.93(16)	C4−N2−C7	112.7(3)
N4−Ag−N6	126.48(15)	C3−N2−Ag	105.3(3)
C4−N2−Ag	112.0(3)	N4−C8−C7	114.1(3)
C7−N2−Ag	100.2(2)	N4−C9−C10	109.8(4)
C12−N4−C8	112.1(4)	C11′−C10−C9	110.9(4)
C12−N4−C9	112.1(5)	C13−C12−N4	128.6(10)
C8−N4−C9	106.5(3)	C12−C13−C14″	108.0(10)
C12−N4−Ag	107.8(6)	O1−S1−O3	116.9(8)
C8−N4−Ag	105.9(2)	O1−S1−O2	114.7(8)
C9−N4−Ag	112.4(2)	O3−S1−O2	113.8(5)
C11−N5−Ag	172.6(5)	O1−S1−C15	94.9(7)
C14−N6−Ag	169.2(8)	O3−S1−C15	108.4(5)
N1−C1−C2	174.8(7)	O2−S1−C15	105.4(6)
C1−C2−C3	111.1(5)	F1−C15−F2	109.8(8)
N2−C3−C2	112.5(4)	F1−C15−F3	109.2(14)
N2−C4−C5	112.9(4)	F2−C15−F3	98.6(15)
C6−C5−C4	109.1(5)	F1−C15−S1	116.8(12)
N3−C6−C5	179.9(9)	F2−C15−S1	120.4(8)
N2−C7−C8	112.7(3)	F3−C15−S1	99.2(7)

[a] Symmetry transformations used to generate equivalent atoms: prime, $x - 1/2, -y + 1/2, z - 1/2$; double prime, $x - 1/2, -y + 1/2, z + 1/2$.

anion-exchanged crystal did not diffract the X-ray beams due to the loss of the single crystallinity. When this anion-exchanged product (NO_3^- solid) or the crystal of **1** was immersed in the aqueous solution of 3 M $LiCF_3SO_3$ for 7 h, all NO_3^- anions were exchanged with $CF_3SO_3^-$.[19] The FT-IR spectrum showed a strong $CF_3SO_3^-$ peak at 1269 cm^{-1}, and the XRPD pattern was coincident with that of **2**. This reversible anion-exchange and the corresponding structural transformation in the crystalline state were able to be performed repeatedly, indicating that the solid **2** is an efficient nitrate sequestering agent. In addition, when the solid **2** was immersed in 3 M $NaClO_4$ for 5 h, the $CF_3SO_3^-$ anion of **2** was quantitatively exchanged with ClO_4^- in the crystalline state, and the structure of **2** was converted to that of **3**. This was verified by EA,[20] FT-IR spectrum,[20] and XRPD patterns (Figure 5). However, the ClO_4^- anion of this solid or the crystal of **3** as prepared could not be exchanged with $CF_3SO_3^-$ even when the solid was immersed in 3 M $LiCF_3SO_3$ solution for 7 days. Similarly, the NO_3^- anion of **1** was exchanged with ClO_4^- when the crystal of **1** was immersed in the aqueous solution of 3 M $NaClO_4$ for 8 h. However, the ClO_4^- anion of the solid **3** was never exchanged with NO_3^-. The results are summarized in Scheme 2. When the solid **2** was immersed in the solution containing both $NaNO_3$ and $NaClO_4$ salts (3 M), $CF_3SO_3^-$ ion of **2** was exchanged only with ClO_4^-, indicating that the ClO_4^- network structure is thermodynamically more stable than the NO_3^- 1-D chain structure. The ion-exchange occurred quantitatively from **1** into **2** and **3** even in dilute solutions such as 0.03 M $LiCF_3SO_3$ and 0.005 M $NaClO_4$, respectively, although it takes a longer time. The quantitative

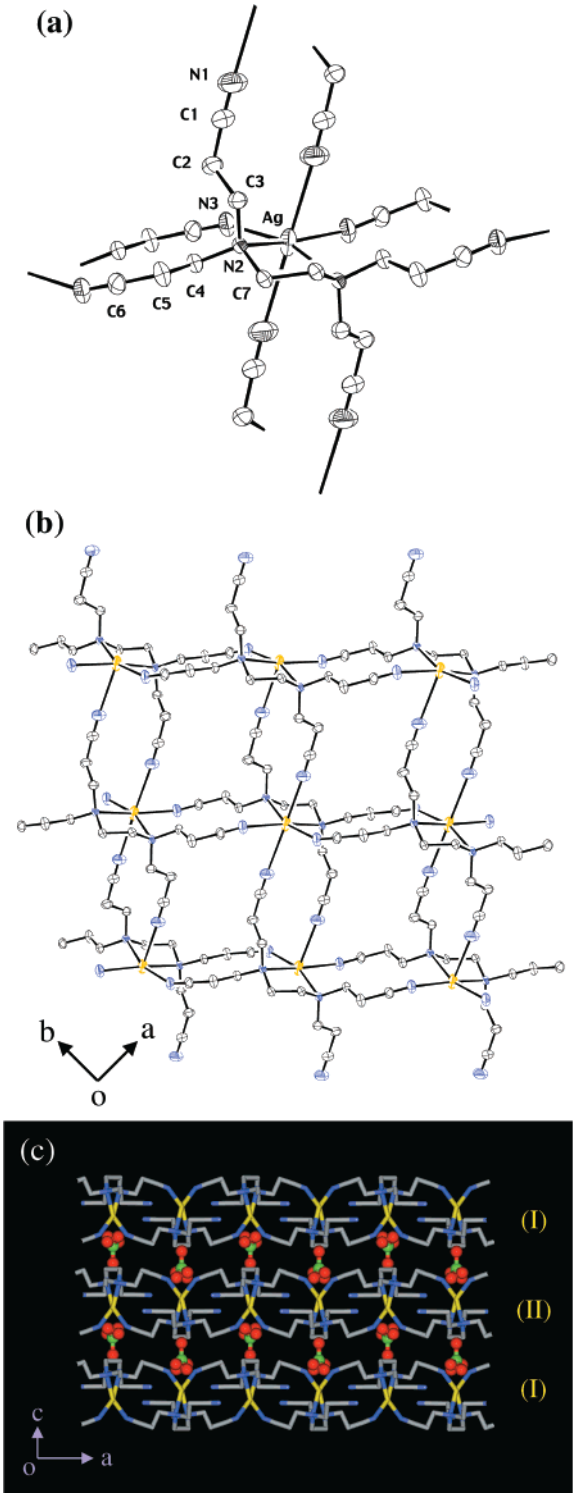

Figure 3. (a) ORTEP drawing of cation of **3** showing the local coordination of Ag(I) and the atomic numbering scheme. The atoms are represented by 40% probable thermal ellipsoid. (b) Extended 2-D structure of **3** (yellow, silver ion; blue, nitrogen; black, carbon). (c) Side view of the packed structure of **3**, showing the position of ClO_4^- ions (yellow, silver ion; blue, nitrogen; gray, carbon; red, oxygen; green, chlorine). The two different series of 2-D layers are indicated as **I** and **II**.

(19) Anal. Calcd for $AgC_{15}H_{20}N_6O_3F_3S$: C, 34.04; H, 3.81; N, 15.88; S, 6.06. Found: C, 33.71; H, 3.89; N, 16.03; S, 5.83.

(20) Anal. Calcd for $AgC_{14}H_{20}N_6ClO_4$: C, 35.06; H, 4.20; N, 17.52. Found: C, 34.69; H, 3.96; N, 17.13. $\nu(ClO_4^-)$: 1084 cm^{-1}.

Table 5. Selected Bond Distances (Å) and Angles (deg) for $[Ag(C_{14}H_{30}N_6)]ClO_4$ (**3**)[a]

Ag−N1a	2.762(6)	C5−C6	1.444(6)
Ag−N2	2.526(3)	N2−C3	1.480(6)
Ag−N3	2.369(4)	N2−C7	1.470(5)
N1−C1	1.133(8)	N3−C6b	1.145(6)
C1−C2	1.458(7)	C7−C7d	1.517(8)
C2−C3	1.535(6)	Cl1−O1	1.374(8)
N2−C4	1.478(5)	Cl1−O2	1.384(11)
C4−C5	1.536(6)	Cl1−O3	1.384(9)
N1a−Ag−N2	91.53(15)	C4−N2−Ag	108.9(2)
N1a−Ag−N2d	96.81(17)	C4−N2−C7	110.0(3)
N1a−Ag−N3	96.94(19)	C6b−N3−Ag	152.6(4)
N1a−Ag−N3d	76.33(17)	C7−N2−Ag	103.3(2)
N1a−Ag−N1c	169.64(12)	N1−C1−C2	178.5(6)
N2−Ag−N2d	75.55(15)	C1−C2−C3	111.1(4)
N2−Ag−N3	92.42(12)	N2−C3−C2	112.4(4)
N2−Ag−N3d	161.93(12)	N2−C4−C5	115.3(3)
N3−Ag−N3d	102.19(19)	C6−C5−C4	109.5(4)
C3−N2−Ag	110.9(2)	N3b−C6−C5	177.2(5)
C3−N2−C4	112.3(3)	N2−C7−C7d	113.8(3)
C3−N2−C7	111.0(3)	O1−Cl1−O2	123.1(15)
O1−Cl1−O3	104.2(7)	O2−Cl1−O3f	118.7(17)
O2−Cl1−O2f	114(3)		

[a] Symmetry transformations used to generate equivalent atoms: a, $-x+1, -y, -z$; b, $-x, -y, -z$; c, $x-1/2, y+1/2, -z$; d, $-x+1/2, -y+1/2, z$; e, $x+1/2, y+1/2, -z$; f, $-x+1/2, -y+3/2, z$.

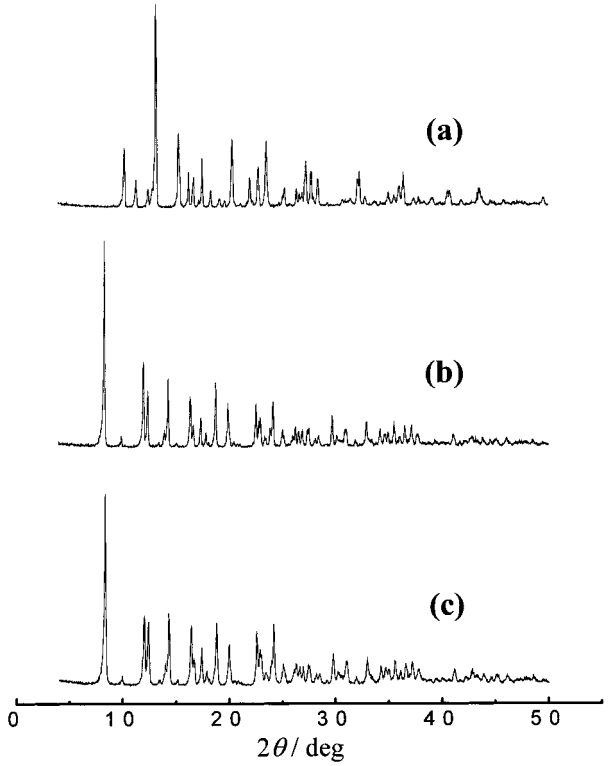

Figure 4. XRPD patterns for (a) **2** as prepared, $[Ag(C_{14}H_{20}N_6)]CF_3SO_3$, (b) solid obtained by immersing **2** in 3 M $NaNO_3$ for 1 h, and (c) **1** as prepared, $[Ag(C_{14}H_{20}N_6)(NO_3)]$.

ion-exchange from **2** into **1** and **3** occurred in the solutions when the salt concentrations were maintained at least 0.02 M $NaNO_3$ and 0.01 M $NaClO_4$, respectively. When the crystals of **1** and **2** were immersed in the aqueous solutions of 3 M NaCl and 2 M $NiSO_4$, they remained intact. However, when the crystal of **3** was immersed in the aqueous solution of NaCl, AgCl and the free ligand (EDTPN) was precipitated, which was indicated by the disappearance of CN stretching at 2264 cm^{-1} and the appearance of a new peak at 2244 cm^{-1} which corresponds to the free cyano group of EDTPN. From the results, the order of

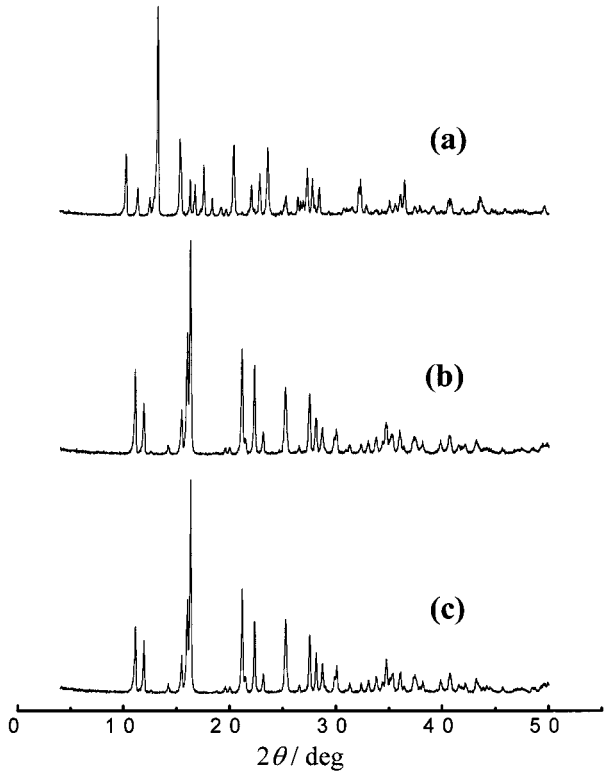

Figure 5. XRPD patterns for (a) **2** as prepared, $[Ag(C_{14}H_{20}N_6)]CF_3SO_3$, (b) solid obtained by immersion of **2** in 3 M $NaClO_4$ for 5 h, and (c) **3** as prepared, $[Ag(C_{14}H_{20}N_6)]ClO_4$.

Scheme 2

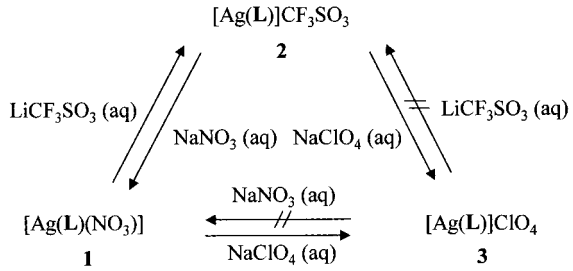

affinity of the solids for anion binding can be assumed as $ClO_4^- > NO_3^- > CF_3SO_3^- > Cl^-$, which is coincident with the Hofmeister series.

The present result is very significant because anion-exchange occurs quantitatively in the crystalline state and the process accompanies the supramolecular structural transformation occurring in the crystalline state, which should give rise to the changes in the cell dimensions (Table 1). There have been a few reports so far of the structural transformation in the crystalline state when the solids were treated with light or solution-phase or gas-phase reagent.[21−23] However, these were observed with the crystals of simple molecules or inorganic solid, instead of the metal−organic supramolecules.

Although the detailed mechanism of the structural transformation in the crystalline state cannot be well understood at this stage, we suggest the mechanism depicted in Scheme 3. When the NO_3^- anion in **1** is exchanged with $CF_3SO_3^-$, the linear chains of **1** are linked together by using one of the three free

(21) Tokitoh, N.; Arai, Y.; Sasamori, T.; Okazaki, R.; Hagase, S.; Uekusa, H.; Ohashi, Y. *J. Am. Chem. Soc.* **1998**, *120*, 433.
(22) Bortun, A. I.; Bortun L. N.; Poojary, D. M.; Xiang, O.; Clearfield, A. *Chem. Mater*. **2000**, *12*, 294.
(23) McKillop, K. L.; Gillette, G. R.; Powell, D. R.; West, R. *J. Am. Chem. Soc*. **1992**, *114*, 5203.

Scheme 3

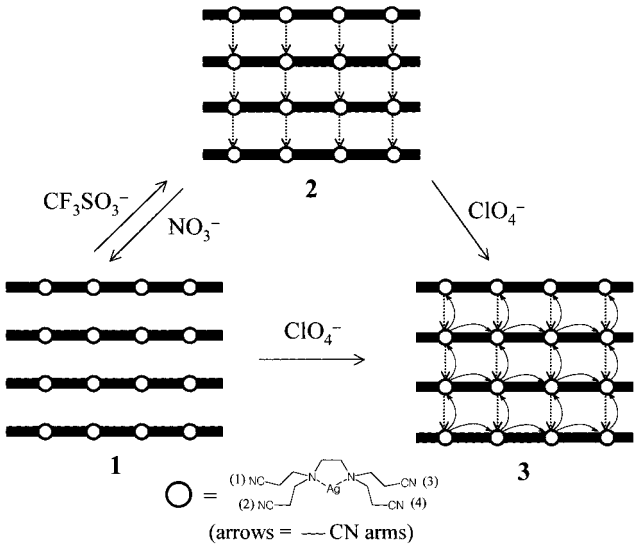

cyano groups of an EDTPN which coordinates a Ag(I) ion of the neighboring chain, which gives rise to a 2-D layer of **2**. When the $CF_3SO_3^-$ anion is exchanged with NO_3^-, the cyano groups linking the 1-D chains are dissociated. When the $CF_3SO_3^-$ anion of **2** is exchanged with ClO_4^-, two free cyano groups of an EDTPN in **2** bind two neighboring Ag(I) ions, one in its own chain and the other in the adjacent chain, which leads to the boxlike 2-D structure of **3**. When the NO_3^- anion in **1** is exchanged with the ClO_4^- anion, three free cyano groups of **1** bind three Ag(I) ions, one Ag(I) ion in its own chain and two Ag(I) ions in two different neighboring chains, which gives rise to the structure of **3**. According to this scheme, the structural transformations among **1**−**3** are possible in the crystalline state, just by the coordination or uncoordination of polynitrile arms of the ligand without significant changes of the location of Ag(I) ions and EDTPN ligands.

Conclusions

Novel supramolecular solids whose structures depend on the counteranion have been constructed from AgX (X = NO_3^-, $CF_3SO_3^-$, and ClO_4^-) and ethylenediaminetetrapropionitrile (EDTPN). The $CF_3SO_3^-$ anion of the solid [Ag(EDTPN)]CF_3SO_3 (**2**) was quantitatively exchanged with NO_3^- and ClO_4^- in the crystalline state, when the crystal of **2** was immersed in aqueous solutions of $NaNO_3$ and $NaClO_4$, respectively. In addition, the NO_3^- anion of **1** was quantitatively exchanged with $CF_3SO_3^-$ and ClO_4^- to form the structures of **2** and **3**, respectively. Interestingly, concomitant with this anion-exchange, the supramolecular structural transformations among **1**−**3** occurred in the crystalline state. We are currently modifying the ligand, such as by changing the length of the nitrile arms to further investigate the anion-exchange ability of the solids and the mechanism of the structural transformations in the solid state.

Acknowledgment. This work was supported by the Korea Science and Engineering Foundation (1999-1-122-001-5) and the Center for Molecular Catalysis.

Supporting Information Available: Figures S1−S3, representing TGA and DSC plots of **1**−**3**, and Tables S1−S18, listing full crystallographic details, fractional atomic coordinates, anisotropic displacement parameters, bond distances and angles, hydrogen atom positions, and bond distances and angles involving hydrogen atoms for **1**−**3** (PDF). An X-ray crystallographic file (CIF). This material is available free of charge via the Internet at http://pubs.acs.org.

JA000642M